

Meson-exchange currents and final-state interactions in quasielastic electron scattering at high momentum transfers

J. E. Amaro,¹ M. B. Barbaro,² J. A. Caballero,³ T. W. Donnelly,⁴ C. Maieron,¹ and J. M. Udias⁵

¹*Departamento de Física Atómica, Molecular y Nuclear, Universidad de Granada, Granada E-18071, Spain*

²*Dipartimento di Fisica Teorica, Università di Torino and INFN, Sezione di Torino, Via P. Giuria 1, I-10125 Torino, Italy*

³*Departamento de Física Atómica, Molecular y Nuclear, Universidad de Sevilla, Apdo.1065, E-41080 Sevilla, Spain*

⁴*Center for Theoretical Physics, Laboratory for Nuclear Science and Department of Physics, Massachusetts Institute of Technology, Cambridge, MA 02139, USA*

⁵*Departamento de Física Atómica, Molecular y Nuclear, Universidad Complutense de Madrid, E-28040, Madrid, Spain*

(Received 30 June 2009; published 13 January 2010)

The effects of meson-exchange currents (MEC) are computed for the one-particle one-hole transverse response function for finite nuclei at high momentum transfers q in the region of the quasi-elastic peak. A semirelativistic shell model is used for the one-particle-emission (e, e') reaction. Relativistic effects are included using relativistic kinematics, performing a semirelativistic expansion of the current operators, and using the Dirac-equation-based (DEB) form of the relativistic mean-field potential for the final states. It is found that final-state interactions (FSI) produce an important enhancement of the MEC in the high-energy tail of the response function for $q \geq 1$ GeV/ c . The combined effect of MEC and FSI goes away when other models of the FSI, not based on the DEB potential, are employed.

DOI: [10.1103/PhysRevC.81.014606](https://doi.org/10.1103/PhysRevC.81.014606)

PACS number(s): 25.30.Fj, 21.60.Cs, 24.10.Jv

In recent years much of the emphasis in studies of inclusive (e, e') scattering was placed on investigations of the scaling properties of the cross section and on the possibility of predicting neutrino cross sections assuming the universality of the scaling function for electromagnetic and weak interactions. An exhaustive analysis of (e, e') world data demonstrated the scaling at energy transfers ω below the quasielastic (QE) peak [1,2], namely the independence of the reduced cross sections on the momentum transfer (first-kind scaling) and on the nuclear target (second-kind scaling) when plotted versus the appropriate scaling variable. It is well known that at energies above the QE peak scaling is violated in the transverse (T) channel by effects beyond the impulse approximation: inelastic scattering [3,4], correlations, and meson-exchange currents (MEC) in both the one-particle one-hole (1p-1h) and two-particle two-hole (2p-2h) sectors [5–8].

In contrast, the available data for the longitudinal (L) response are compatible with scaling throughout the QE region and permitted [9] the extraction of a phenomenological scaling function f_L . In recent work [10–12] it was shown that only a few models [the relativistic mean field (RMF), the semirelativistic (SR) approach with Dirac-equation-based (DEB) and a “BCS-like” model] are capable of reproducing the detailed shape of f_L , while other models fail to reproduce the long tail appearing at high ω . These models effectively account for the major ingredients needed to describe the (e, e') responses for intermediate-to-high momentum transfers, namely relativistic effects and an appropriate description of the effective final-state interactions (FSI).

Approximate treatments of these two ingredients are also possible using SR models, which have the advantage of permitting the use of standard nonrelativistic techniques when correctly extrapolated to high values of q . In this article we use the approach of Refs. [11,13] where a specific SR expansion of the electroweak single-nucleon current was

used in a continuum shell-model description of electron and neutrino inclusive QE scattering from closed-shell nuclei. In the model the (nonrelativistic) hole states are taken to be states in a Woods-Saxon potential, while the final particles in the continuum are described with the DEB form of the RMF plus the so-called Darwin term. This may raise the issue of spurious nonorthogonality contributions to the responses [14,15]. However, as shown in Ref. [13], the present SR model gives results that are very similar to the RMF, where the same potential is used for initial and final states and thus there is no orthogonality problem. This allows us to conclude that the nonorthogonality effects are very small. In previous studies it was shown that the T response computed in impulse approximation has the same scaling properties as the L response. The deviations from scaling observed in data for the T response are usually ascribed to mechanisms beyond the one-particle emission channel, specifically, two-particle emission, delta excitation, and other inelastic processes.

In this article we focus on a study of the MEC contributions in the 1p-1h transverse QE response at high-momentum transfers. The MEC here are two-body contributions, which at the 1p-1h level occur coherently with the familiar one-body contributions; the former are depicted in the diagrams of Fig. 1. Most of MEC studies performed for low-to-intermediate momentum transfers [6,7,16–20] showed a small reduction of the total response at the peak. These are produced mainly via the Δ current [diagrams (d) through (g)—excitation of a virtual Δ , which subsequently decays, exchanging a pion with a nucleon in the Fermi sea], while the seagull (S) and pion-in-flight (P) currents [diagrams (a), (b), and (c), respectively] give a net positive but smaller contribution [21]. Specifically, the destructive interference between the familiar one-body and two-body contributions yields a 12% reduction of the total at $q = 500$ MeV/ c , rising to about 20% at $q = 1$ GeV/ c . The shape of the T response does not change too

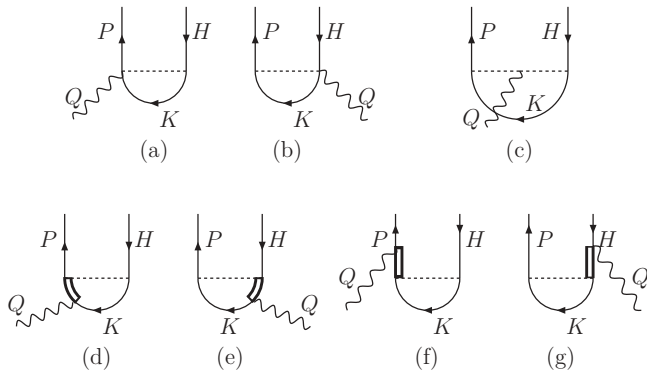


FIG. 1. One-particle (P) one-hole (H) MEC diagrams considered in the present study. Diagrams (a) and (b) correspond to the seagull, (c) to the piononic, and (d) through (g) to the Δ current, respectively. The intermediate particle K corresponds to a sum over occupied holes in the shell-model core.

much for such kinematics, resulting in only small scaling violations in the total T channel. Similar effects were also found at higher momentum transfers using a relativistic Fermi gas (RFG) model [5,6]. The same trend is confirmed by the results of the present study for $q = 1$ GeV/c, as shown in the upper panel of Fig. 2: here the T response obtained using the DEB model with and without MEC is displayed.

However, the behavior changes for higher values of q , as shown in the lower panels of Fig. 2. For the DEB + MEC approach the reduction of the response in the peak region due to MEC is now accompanied by an increase of the tail in the high- ω region, where an enhancement of R_T appears as a bump, producing a drastic change from the usual QE peak shape. Therefore, one expects a large violation of first-kind scaling in this region even when considering only the $1p$ - $1h$ T response. The amount of violation increases with q and for $q = 1.5$ GeV/c a plateau-like shape is obtained. However, such peculiar behavior for high q is not observed when using a Woods-Saxon (WS) potential for the final states. The reason is that the MEC bump appears in the high-energy region where the WS results are very small and therefore not observable in the figure, whereas the DEB potential gives rise to a long tail, which emphasizes the effects occurring at large ω .

From Fig. 1 it also appears that the seagull and pion-in-flight diagrams very weakly affect R_T while the largest MEC contribution comes from the interference term between one-body and two-body Δ currents. The SR Δ current used in this work is taken from Ref. [22] and includes a static propagator for the intermediate Δ . One might think that the static approximation should not be adequate for high energies and momentum transfers. The problem of using a dynamical Δ propagator is very demanding in the shell model. However, a comparison was performed in Ref. [22] in the framework of the Fermi gas between the SR approach with several prescriptions for the Δ propagator and the RFG of Ref. [6] where the dynamical Δ propagator was treated exactly. It was shown that among these the static approximation gives the closest results to the exact RFG for $q < 1$ GeV/c. For the present study we extended the SR model for the Δ current to $q = 1.5$ GeV/c.

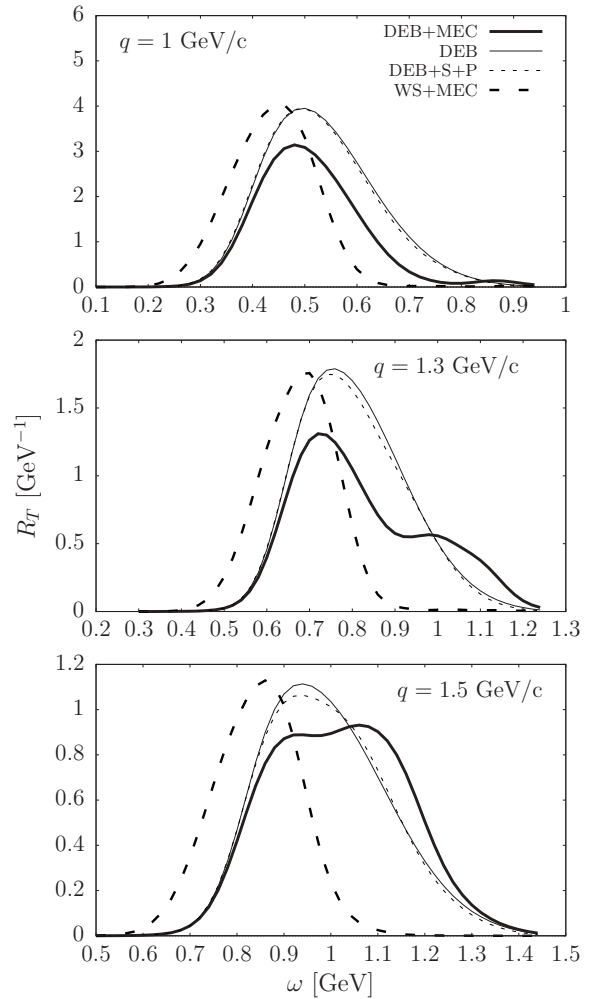


FIG. 2. Transverse response for ^{12}C versus ω for three values of q . The results with the DEB potential including the full MEC (thick solid lines), the seagull (S) and pion-in-flight (P) currents (thin-dashed lines) and only the one-body current (thin solid lines) are displayed. Also shown are the results corresponding to the Woods-Saxon potential with the full MEC contribution (thick-dashed lines).

We first checked that at these high values of q the static approximation is still valid, as demonstrated in Fig. 3 where we show the interference between the Δ and one-body (OB) current in the T response. Indeed the SR Fermi gas results are seen to be very close to the RFG ones even for q as high as 1.5 GeV. In the same figure we also show the SR shell-model results using the WS potential. The RFG and WS are very similar, except for the kinematical region where the RFG is zero. Finally, in Fig. 3 we show the results obtained using the DEB potential, which produces a significant hardening of the response and an oscillatory behavior at high q . A change of sign appears above $\omega \simeq 1$ GeV and is responsible for the MEC bump observed in Fig. 2. By closer inspection of Fig. 3, a change of sign can also be observed in the WS results for the same energy, although the response is so small in that region that the effect is negligible.

The change of sign of the Δ contribution and the associated bump in the response function are produced by the pion

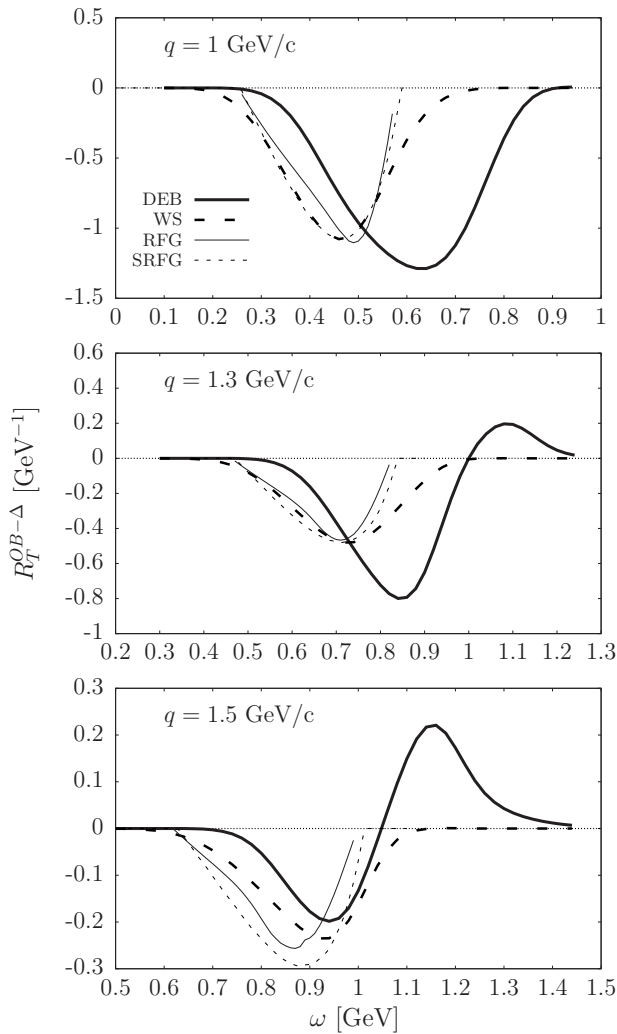


FIG. 3. The transverse response corresponding to the interference between one-body and Δ currents is shown for the DEB (thick-solid lines) and Woods-Saxon (thick-dashed lines) potentials, the relativistic Fermi gas (thin-solid lines) and the SR Fermi gas (thin-dashed lines).

propagator. In the shell-model studies we use a dynamical pion propagator (i.e., the exact one), which depends on the energy of the exchanged pion. The present computations are done in position space and the pion propagator is Fourier-Bessel transformed through a multipole expansion (but is still energy dependent). For pion energies above the pion mass a pole occurs in the Fourier integral, giving rise to a change of sign in the Δ contribution (note that the pole is treated as a principal value, hence no real pions are being produced). Since in all of the MEC diagrams there is an exchanged pion, one should also expect a bump in the seagull and pionic contributions. In fact those bumps are present but small. The total MEC contribution has the same oscillatory behavior as the Δ current, contributing to the MEC bump in the high ω tail in Fig. 2. The largest contribution comes from the Δ current, while the seagull plus pionic currents are very small and they both show a similar structure with the expected oscillation and bump. The seagull and pionic contributions are opposite in sign and

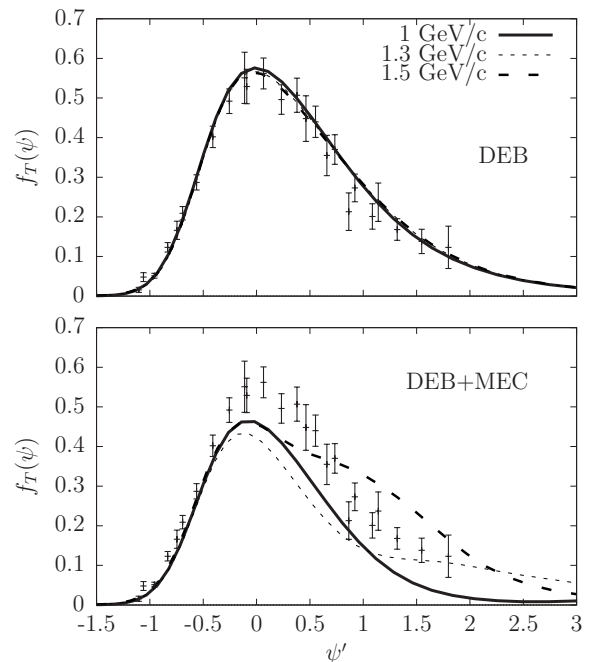


FIG. 4. Transverse scaling function computed with and without MEC as a function of the scaling variable ψ' computed as in Ref. [11]. The experimental data from Ref. [9].

almost cancel out; accordingly, their net contribution is small and the Δ dominates the MEC.

The scaling violation of the 1p-1h transverse response by the MEC is shown in Fig. 4, where the transverse scaling function f_T is plotted as function of the scaling variable ψ' [11] for $q = 1, 1.3$, and 1.5 GeV/c. The DEB response functions scale without MEC, reproducing the asymmetrical shape of the the longitudinal scaling function experimental data. Scaling is clearly broken for $\psi' > 0$ when MEC are taken into account, while it is still valid for $\psi' < 0$.

Further insight into the enhancement of MEC from the pion dynamical propagator is illustrated in Fig. 5, where we compare the full calculation with the DEB results using a static pion propagator. The oscillation and bump disappear when the static pion propagator is used and the MEC contribution is significantly reduced. A similar effect is also observed with a WS potential, even if here the MEC bump is absent. Concerning the effect of the DEB potential compared with the WS results, we see that in both cases (static or dynamic pions) a hardening of the response is observed, although in the dynamical case an additional change of sign is produced. This change of sign is related to the oscillatory behavior of the pion propagator in coordinate space for high pion energies, in contrast to its exponential Yukawa-type behavior in the static case. Unfortunately, a simple estimate of the ω value where the bump appears is not possible since that value does not depend on the kinematics in a trivial way. In fact the pion propagator appears inside an involved integration containing the nuclear wave functions over an internal coordinate that is not attached to the pion in the diagrams of Fig. 1. A more detailed investigation of the physical origin and energy

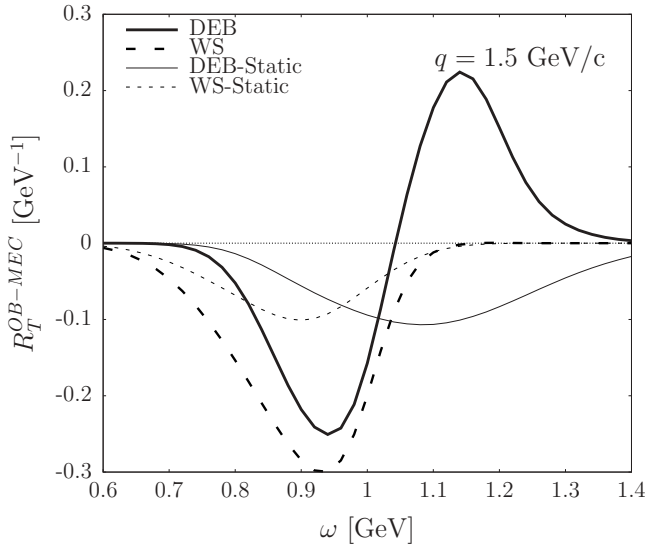


FIG. 5. Interference one-body/two-body transverse response obtained with the DEB (solid line) and WS (dashed line) potentials. The thick lines correspond to the exact dynamical pion propagator, the thin lines to the static approximation.

dependence of these results is currently being pursued and will be reported elsewhere.

In summary, in the present work we computed the MEC effects in the transverse $1p-1h$ response for high-momentum transfers in a continuum SR shell model using the DEB potential for the final states. The MEC are found to give an important contribution to the response, which is negative at the peak and positive in the high-energy tail due to a change

of sign of the MEC contribution for transferred energies above 1 GeV. These results confirm the MEC as an important source of scaling violations in the T response at high q . The MEC bump is only predicted when the FSI produce a dynamical enhancement of the high-energy tail of the responses (as in the case of the DEB potential) and when this enhancement works in concert with the dynamical pion propagator. Finally, let us mention that in this article, as in past work (see Ref. [7] for details), we use a monopole parametrization for the πNN and $\pi N\Delta$ form factors, giving a smooth dependence on the energy of the pion. Different prescriptions will modify slightly the present results, but they will remain qualitatively the same without changing our conclusions.

Although the effects shown in the present work are usually masked by other contributions appearing at the kinematical region considered (Δ production, two-particle emission, etc.) and cannot be separately observed in inclusive experiments, we show here that they are not negligible. This has important implications for neutrino reaction studies [23], where the contributions reported in the present work must, of course, also be included.

ACKNOWLEDGMENTS

This work was partially supported by DGI (Spain) Grant Nos. FIS2008-01143, FPA2006-13807-C02-01, FIS2008-04189, and FPA2007-62216, by the Junta de Andalucía, by the INFN-MEC collaboration agreement, project “Study of relativistic dynamics in neutrino and electron scattering,” the Spanish Consolider-Ingenio 2000 programed CPAN (CSD2007-00042), and part (TWD) by the US Department of Energy under cooperative agreement DE-FC02-94ER40818.

-
- [1] T. W. Donnelly and I. Sick, *Phys. Rev. Lett.* **82**, 3212 (1999).
- [2] T. W. Donnelly and I. Sick, *Phys. Rev. C* **60**, 065502 (1999).
- [3] L. Alvarez-Ruso, M. B. Barbaro, T. W. Donnelly, and A. Molinari, *Nucl. Phys.* **A724**, 157 (2003).
- [4] M. B. Barbaro, J. A. Caballero, T. W. Donnelly, and C. Maieron, *Phys. Rev. C* **69**, 035502 (2004).
- [5] J. E. Amaro, M. B. Barbaro, J. A. Caballero, T. W. Donnelly, and A. Molinari, *Nucl. Phys.* **A697**, 388 (2002).
- [6] J. E. Amaro, M. B. Barbaro, J. A. Caballero, T. W. Donnelly, and A. Molinari, *Nucl. Phys.* **A723**, 181 (2003).
- [7] J. E. Amaro, M. B. Barbaro, J. A. Caballero, T. W. Donnelly, and A. Molinari, *Phys. Rep.* **368**, 317 (2002).
- [8] A. De Pace, M. Nardi, W. M. Alberico, T. W. Donnelly, and A. Molinari, *Nucl. Phys.* **A741**, 249 (2004).
- [9] C. Maieron, T. W. Donnelly, and I. Sick, *Phys. Rev. C* **65**, 025502 (2002).
- [10] J. A. Caballero, J. E. Amaro, M. B. Barbaro, T. W. Donnelly, C. Maieron, and J. M. Udias, *Phys. Rev. Lett.* **95**, 252502 (2005).
- [11] J. E. Amaro, M. B. Barbaro, J. A. Caballero, T. W. Donnelly, and J. M. Udias, *Phys. Rev. C* **75**, 034613 (2007).
- [12] M. B. Barbaro, R. Cenni, T. W. Donnelly, and A. Molinari, *Phys. Rev. C* **78**, 024602 (2008).
- [13] J. E. Amaro, M. B. Barbaro, J. A. Caballero, T. W. Donnelly, and C. Maieron, *Phys. Rev. C* **71**, 065501 (2005).
- [14] J. I. Johansson, H. S. Sherif, and F. Ghodoussi, *Nucl. Phys.* **A665**, 403 (2000).
- [15] S. Boffi, F. Cannata, F. Capuzzi, C. Giusti, and F. D. Pacati, *Nucl. Phys.* **A379**, 509 (1982).
- [16] W. M. Alberico, T. W. Donnelly, and A. Molinari, *Nucl. Phys.* **A512**, 541 (1990).
- [17] M. Kohno and N. Otsuka, *Phys. Lett.* **B98**, 335 (1981).
- [18] M. J. Dekker, P. J. Brussaard, and J. A. Tjon, *Phys. Lett.* **B289**, 255 (1992).
- [19] A. Fabrocini, *Phys. Rev. C* **55**, 338 (1997).
- [20] V. Van der Sluys, J. Ryckebusch, and M. Waroquier, *Phys. Rev. C* **51**, 2664 (1995).
- [21] J. E. Amaro, A. M. Lallena, and G. Co, *Nucl. Phys.* **A578**, 365 (1994).
- [22] J. E. Amaro, M. B. Barbaro, J. A. Caballero, and F. Kazemi Tabatabaei, *Phys. Rev. C* **68**, 014604 (2003).
- [23] Y. Umino, J. M. Udias, and P. J. Mulders, *Phys. Rev. Lett.* **74**, 4993 (1995).